

Initial growth stages of epitaxial BaTiO₃ films on vicinal SrTiO₃:Nb (001) substrates

A. Visinoinu, M. Alexe, H. N. Lee, D. N. Zakharov, A. Pignolet, D. Hesse, and U. Gösele
Max Planck Institute of Microstructure Physics, D-06120 Halle (Saale), Germany.

ABSTRACT

The growth mechanism of epitaxial BaTiO₃ films on vicinal Nb-doped SrTiO₃ (SrTiO₃:Nb) (001) substrate surfaces was studied in terms of surface morphology, crystalline orientation, microstructure, and film/substrate interface. Well-oriented BaTiO₃ thin films were grown on SrTiO₃ substrates with well-defined terraces by pulsed laser deposition. The regularly terraced TiO₂-terminated surfaces of vicinal SrTiO₃:Nb (001) substrates were prepared by a definite chemical and thermal treatment. Under our conditions, BaTiO₃ seems to grow with a layer-then-island (Stranski-Krastanov) growth mechanism. In order to investigate the orientation and crystallinity of the BaTiO₃ films, x-ray diffraction and high-resolution transmission electron microscopy were performed. Ferroelectricity of the BaTiO₃ films was proved by electrical measurements performed on Pt/BaTiO₃/SrTiO₃:Nb heterostructures.

INTRODUCTION

BaTiO₃ is considered to be the prototype of perovskite ferroelectrics [1]. Considerable attention has been given to the properties of grown films explaining them in terms of advanced growth, while the initial stages of film growth and the growth mechanisms are so far not studied in detail. The classical theory of film growth distinguishes three growth mechanisms: layer-by-layer growth (Frank-van-der Merwe), island growth (Volmer-Weber), and layer-then-island growth (Stranski-Krastanov), depending on the surface energies of film and substrate, as well as of the film/substrate interface energy [2].

Pulsed laser deposition (PLD) has become an important technique to produce high-quality multicomponent thin films including ferroelectric, high-temperature superconducting, electro-optic, and optical films [3]. The growth of BaTiO₃ films by PLD on different substrates has been observed to follow different mechanisms, e.g. layer-by-layer growth on SrTiO₃ (001) [4], island growth on MgO (001) [5]. Layer-by-layer growth has been reported to be a possible growth mechanism by theoretical electronic structure calculations taking into account the surface charge neutrality [6].

This paper presents an experimental study of initial stages of the epitaxial BaTiO₃ film growth on SrTiO₃ (001) substrates by PLD. Our motivation for this work is a better understanding of the initial growth mechanism of BaTiO₃ (tetragonal: $a = b = 3.994 \text{ \AA}$ and $c = 4.038 \text{ \AA}$) films. SrTiO₃ (cubic: $a_c = 3.905 \text{ \AA}$) substrates have been chosen because of the low lattice mismatch $(a_{\text{film}} - a_{\text{substrate}}) / a_{\text{substrate}} = 2.28\%$. This work is to be considered in the general frame of improvement of the dielectric properties of BaTiO₃ films by replacing them with BaTiO₃/SrTiO₃ superlattices [7].

EXPERIMENTAL DETAILS

Epitaxial BaTiO₃ films were grown on SrTiO₃:Nb (001) substrates with a Nb concentration of 0.1%. In order to properly study the growth mechanism of the BaTiO₃ films, a well-defined surface morphology is required as a reference before any deposition. Therefore, as-received SrTiO₃:Nb miscut substrates were subjected to a specific procedure consisting of two steps, viz. a chemical treatment and a thermal treatment. SrTiO₃ substrates were etched for 30 s in a buffered NH₄F-HF solution (BHF) having a pH of 4.5, cleaned for about 1 min in deionized water and dried in a nitrogen stream. Then, the substrate surfaces were re-crystallized by a 10 min post-anneal at 1200 °C in air. The surface morphology was investigated by atomic force microscopy (AFM) (Digital Instruments D5000) working in tapping mode and using an ultrasharp silicon tip with a resonance frequency of about 350 kHz. Further on, PLD was used to grow BaTiO₃ thin films. A KrF excimer laser ($\lambda = 248$ nm) is focused at a 45° angle onto a ceramic stoichiometric BaTiO₃ target. The deposition was performed at a substrate temperature of 700 °C and at an oxygen pressure of 0.2 mbar using a laser energy of 600 mJ and a repetition rate of 1 Hz. After deposition, the samples were cooled down in high vacuum. The microstructure of the BaTiO₃ thin films and the BaTiO₃/SrTiO₃ interface were investigated by cross section high-resolution transmission electron microscopy (HRTEM) in a JEOL 4010 electron microscope at a primary beam energy of 400 keV. In order to study the crystallographic orientation, x-ray diffraction (XRD) θ - 2θ scans, pole-figures, and ϕ scans were performed using a Philips X'Pert MRD four-circle diffractometer with Cu K α radiation and a parallel plate collimator in front of the detector with a 2θ resolution of 0.1°. Pt electrodes with 100 nm thickness and 0.15 mm diameter were deposited by rf-sputtering through a metallic mask at room temperature. Electrical characterization was performed using a TF Analyzer 2000 ferroelectric tester (AixACCT) and a Hewlett Packard HP 4195A impedance analyzer.

RESULTS AND DISCUSSION

Vicinal surfaces of well-polished (001)-oriented SrTiO₃:Nb single crystal substrates were obtained after a specific cleaning process which consists of both a chemical and a thermal treatment in order to obtain smooth reproducible surfaces and to control their roughness. Vicinal substrates with 0.1°, 0.5°, 1°, and 1.5° miscut angles were subjected to these procedures. The effect of these treatments on the morphology of the substrate surface was studied by AFM and is summarized in figure 1 for the 0.1° miscut substrate. The initial state of the as-received SrTiO₃:Nb substrates [Fig. 1(a)] consists of a rough surface with a roughness of 0.2 nm to 0.4 nm which corresponds to the half and full lattice parameter of SrTiO₃, respectively. This suggests the existence of both possible surface terminations of SrTiO₃, i.e. SrO and TiO₂. To study the initial growth stages of BaTiO₃ films, SrTiO₃:Nb substrates should be single terminated in order to impose only one possible stacking sequence of the deposited material [8]. Kawasaki *et al.* [9] showed that by dissolving one of the atomic layers controlling the pH of the BHF solution, the surface becomes single terminated. Therefore, we performed a chemical etching process in

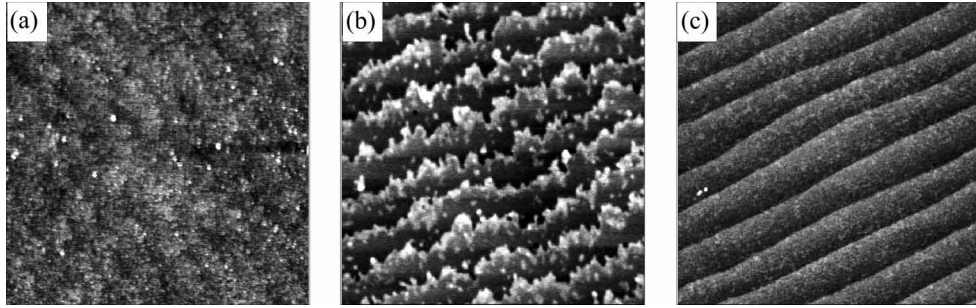


Figure 1. AFM images ($2 \times 2 \mu\text{m}^2$ area, 1 nm in height from black to white) of 0.1° miscut SrTiO_3 (001) substrates, (a) as-received, (b) after BHF etching, (c) after etching and annealing.

which SrO-terminated surface sections are dissolved and the final surface is TiO_2 -terminated [Fig. 1(b)], as revealed by AFM profiles. No differences were observed by varying the etching time from several seconds to 1 min. However, atomically flat surfaces of the SrTiO_3 (001) substrates were not achieved by only a chemical treatment. Therefore, we performed a second treatment consisting of a 10 min post-anneal at 1200°C . Finally, well-defined terraces of about 0.4 nm height and 150 - 250 nm width were obtained after both chemical and thermal treatments [Fig. 1(c)]. Increasing the miscut angle of the SrTiO_3 substrates, the density of terraces increases as well. Vicinal 0.1° miscut SrTiO_3 substrates were chosen for the experiments described here.

In order to study the initial growth mechanism of BaTiO_3 , a sequence of BaTiO_3 thin films with nominal thicknesses ranging from 0.6 nm to 320 nm was deposited on vicinal (001) $\text{SrTiO}_3:\text{Nb}$ substrates. In the early growth stage, after a deposition of 0.2 min, a uniform layer about 1 nm in nominal thickness consisting of small grains covers the substrate surface, the terraces still being visible [Fig. 2(a)]. After 1 min of deposition, small grains appear to “decorate” the previously uniform layer [Fig. 2(b)]. The nominal thickness is about 5 nm. After 5 min of deposition, the density of small grains increases (25 nm nominal thickness). After a deposition of 8 min, large grains of about 100 nm in lateral size develop on the surface

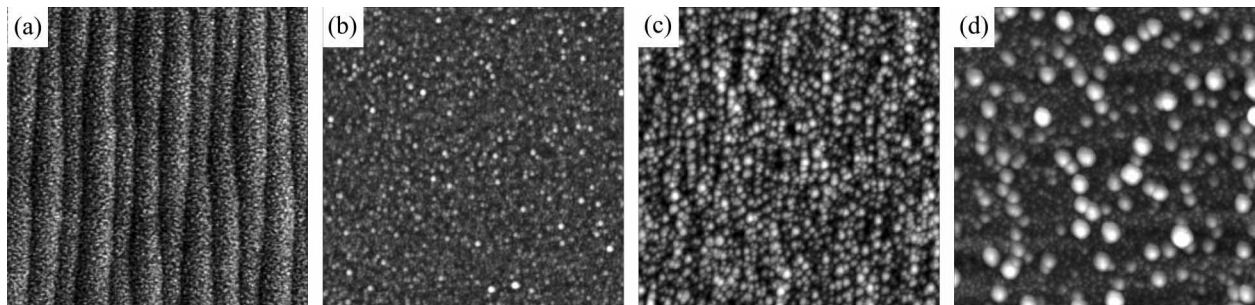


Figure 2. AFM images ($2 \times 2 \mu\text{m}^2$ area, 20 nm in height from black to white) of BaTiO_3 films with (a) 1 nm, (b) 5 nm, (c) 40 nm, and (d) 260 nm nominal thickness.

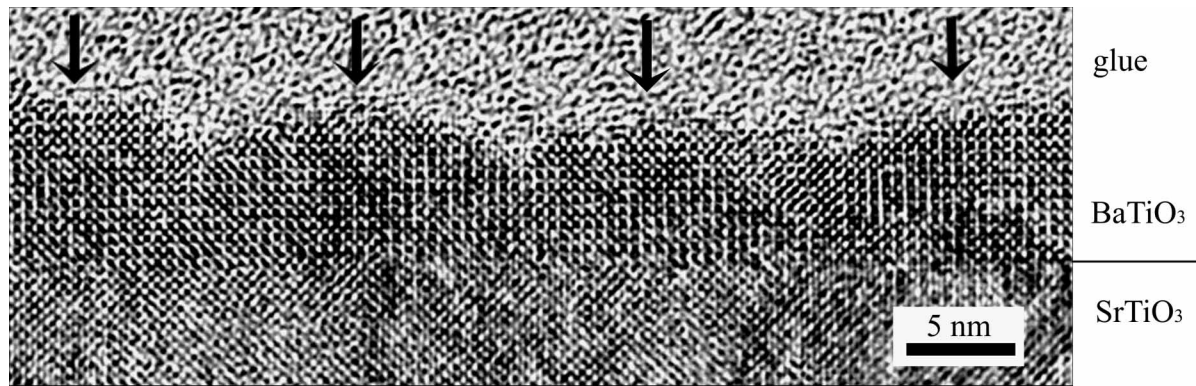


Figure 3. Cross section HRTEM image demonstrating the layer-then-island growth mode of a BaTiO₃ film on a SrTiO₃ layer of a BaTiO₃/SrTiO₃ multilayer stack.

instead of the small ones, at a nominal thickness of about 40 nm [Fig. 2(c)]. In figure 2(d), two different sizes of grains are visible in a film deposited for 30 min (260 nm thickness). From this thickness on, the average in-plane size of the larger grains does not significantly increase with a further increasing in film thickness, while the root mean square roughness of the film increases from 0.17 nm to 4.6 nm when the nominal film thickness increases from 0.6 nm to 320 nm. Due to coalescence, the small grains become the nucleation sites for the large grains of about 100 nm in lateral size which develop upon further film deposition. All these results suggest a layer-then-island (Stranski-Krastanov) growth mechanism of BaTiO₃ films on SrTiO₃ substrates under our deposition conditions.

While AFM imaging of the surfaces allows to study the surface morphology, cross-section TEM imaging reveals the relationship between the surface roughness and the grain-like structure of the BaTiO₃ thin films. A cross-sectional HRTEM view of a BaTiO₃ film of about 5 nm thickness on SrTiO₃, seen along the [010] SrTiO₃ zone axis, is shown in Fig. 3. The film/substrate interface is well-defined and sharp. Several grains with a height of four to five BaTiO₃ unit cells begin to grow on top of a thin continuous layer about 4 nm thick, which covers the substrate surface. The island height corresponds to a peak-to-valley height of 1.4 - 1.8 nm

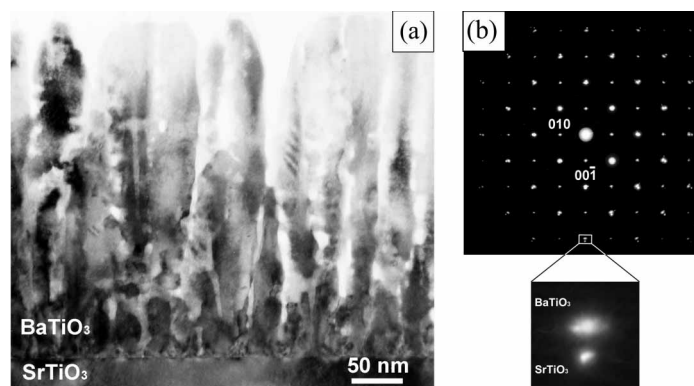


Figure 4. Cross section TEM image and diffraction pattern of a 320 nm thick BaTiO₃ film grown on a SrTiO₃:Nb substrate.

measured by AFM. A columnar structure was observed for a 320 nm BaTiO₃ thick film [Fig. 4(a)]. The diffraction pattern taken from the interface region shows reflections from both BaTiO₃ and SrTiO₃ [Fig. 4(b)]. It is well-known that BaTiO₃ has a tetragonal structure at room temperature, but the difference between lattice parameters a and c is only about 0.044 Å. Unfortunately, due to this small difference it was not possible to distinguish the a - and c -domains of the BaTiO₃ film in HRTEM images. Films of a thickness up to 6 nm reveal no defects and a sharp interface with the substrate. Overall, our conclusion that our BaTiO₃ films grow by a layer-then-island growth mechanism is sustained by the TEM investigation.

The crystallinity of the BaTiO₃ films was investigated by x-ray diffraction θ - 2θ scans, pole figures, and ϕ scans. Figure 5(a) presents a θ - 2θ scan of a 40 nm thick BaTiO₃ film grown on a (001) SrTiO₃:Nb substrate. Again it was impossible to distinguish between the a -orientation and the c -orientation of BaTiO₃ because the related difference in 2θ is less than 1°. ϕ -scan measurements were performed using the 110 ($2\theta = 31.64^\circ$, $\psi = 45^\circ$) and the 211 ($2\theta = 56.25^\circ$, $\psi = 35^\circ$) reflections of BaTiO₃, and for the 222 ($2\theta = 86.2^\circ$, $\psi = 55^\circ$) reflection of SrTiO₃ [Fig. 5(b)]. Four diffraction peaks with a fourfold symmetry were observed showing that the BaTiO₃ thin film has a very good in-plane orientation. The full-width at half maximum (FWHM) in the rocking curve of the BaTiO₃ 200/002 peak shows values ranging from 0.24° to 0.52° which confirm the good crystallinity of the BaTiO₃ films.

In order to study the dielectric properties of the BaTiO₃ thin films, macroscopic measurements were performed on Pt/BaTiO₃/SrTiO₃:Nb heterostructures. The relative dielectric constant and the dielectric loss at room temperature measured at 10 kHz are 615 and 0.04, respectively. The remanent polarization and the coercive field are 1.53 $\mu\text{C}/\text{cm}^2$ and 36.4 kV/cm, respectively, for a maximum applied field of 100 kV/cm. Local piezoelectric measurements confirmed the ferroelectric behavior, as well as the presence of an initial imprint in BaTiO₃ thin films on SrTiO₃:Nb substrates.

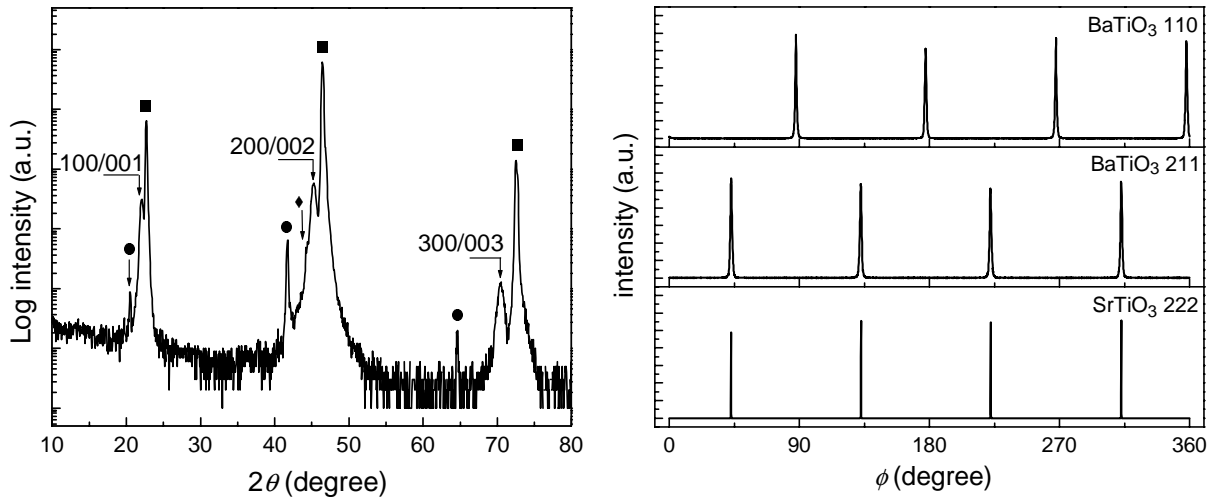


Figure 5. X-ray diffraction (a) θ - 2θ scan and (b) ϕ -scan of a BaTiO₃ film of 40 nm in thickness on a SrTiO₃ (001) substrate. The peaks labelled as (■) are the SrTiO₃ proper substrate peaks, while those labelled as (●) and (▼) are the substrate peaks originating from the remaining Cu K β radiation and from the W L α radiation, respectively.

CONCLUSIONS

The initial growth stages of BaTiO₃ films were studied by AFM, TEM, and XRD measurements. Epitaxial BaTiO₃ thin films were grown by PLD on SrTiO₃:Nb (001) substrates. Vicinal substrate surfaces with well-defined terraces were prepared by both etching and annealing treatments. In order to study the crystallinity of the deposited films, XRD θ - 2θ scans, pole figures, and ϕ scans were performed. Under our deposition conditions, the BaTiO₃ film seems to grow by a layer-then-island (Stranski-Krastanov) growth mechanism. In the early growth stage, a uniform grainy layer of about 5 nm in thickness covers the substrate surface. Increasing the film thickness, individual grains begin to grow. Their density increases on further deposition. Due to coalescence, these small grains become the nucleation sites for the large grains of about 100 nm in lateral size which develop upon further film deposition. The columnar structure of the thicker BaTiO₃ films follows the grainy structure of the thinner BaTiO₃ layer. Up to 6 nm in thickness, BaTiO₃ films showed no defects in their structure. The remanent polarization and coercive field of Pt/BaTiO₃/SrTiO₃:Nb heterostructures are 1.53 $\mu\text{C}/\text{cm}^2$ and 36.4 kV/cm, respectively. The relative dielectric constant and the dielectric loss at room temperature are about 615 at 10 kHz and 0.04, respectively.

ACKNOWLEDGEMENT

The authors would like to thank Dr. C. Harnagea for the local piezoelectric measurement.

REFERENCES

1. M. E. Lines and A. M. Glass, in *Principles and Applications of Ferroelectrics and Related Materials*, edited by W. Marchall and D.H. Wilkinson (Clarendon Press, Oxford, 1977), p. 245.
2. J. S. Horwitz and J. S. Sprague, in *Pulsed Laser Deposition of Thin Films*, edited by D. B. Chrisey and G. K. Hubler (Wiley, New York, 1994), p. 231.
3. O. Auciello, in *Handbook of Crystal Growth*, edited by D. T. J. Hurle (Elsevier Science, Amsterdam, 1994), Vol. 3A, p. 367.
4. H. Tabata, H. Tanaka, and T. Kawai, *Appl. Phys. Lett.* **65**, 1970 (1994).
5. M. G. Norton, and C. B. Carter, *J. Mater. Res.* **5**, 2762 (1990).
6. Y. S. Kang, I. Tanaka, H. Adaki, and S. J. Park, *Jpn. J. Appl. Phys.* **35**, L1614 (1996).
7. H. Tabata, H. Tanaka, T. Kawai, and M. Okuyama, *Jpn. J. Appl. Phys.* **34**, 544 (1995).
8. G. Koster, A. J. H. M. Rijnders, D. H. A. Blank, and H. Rogalla, *Physica C* **339**, 215 (2000).
9. M. Kawasaki, K. Takahashi, T. Maeda, R. Tsuchiya, M. Shinohara, O. Ishiyama, T. Yonezawa, M. Yoshimoto, and H. Koinuma, *Science* **266**, 1540 (1994).